J. Fluid Mech. (1980), *vol.* 96, *part* 3, *pp.* 481–492
Printed in Great Britain

On the secondary instability in inclined air layers

By DOUGLAS W. RUTH,† G. D. RAITHBY AND K. G. T. HOLLANDS

Department of Mechanical Engineering, University of Waterloo, Ontario, Canada

(Received 9 August 1978 and in revised form 2 July 1979)

The heat transfer across an inclined air layer in the longitudinal roll regime often falls below expected values. A companion paper (Ruth *et al.* 1980) presents the heat transfer measurement and flow visualization observations; the present paper discusses the mechanisms which are thought to be responsible for this anomalous behaviour and formulates a simple model which correlates the results of our previous study and that of Hart (1971). The observed suppression of heat transfer below values expected for pure longitudinal roll motion is explained in terms of a shear instability. A stabilizing mechansim, which would restore the longitudinal rolls at higher Rayleigh numbers, is described; the return of the heat transfer to expected levels at higher Rayleigh numbers is ascribed to this mechanism. Comparisons are made between the results of the present model and the analyses of Clever & Busse (1977).

1. Introduction

The problem of interest here is the flow in, and heat transfer across, a layer of air contained between flat, parallel, isothermal plates that are inclined at an angle ϕ to the horizontal. For $0° < \phi \lesssim 70°$, where $\phi = 0°$ is horizontal, a 'top-heavy' instability causes longitudinal rolls to form for Rayleigh numbers, Ra, above a critical value Ra_c. The existence of longitudinal rolls was shown by Clever (1973), for large Prandtl numbers, Pr, and by Hollands *et al.* (1976), for arbitrary Pr, to imply a 'scaling' of the heat transfer. That is, the Nusselt number at arbitrary ϕ can be obtained from data or equations applicable to the horizontal case by replacing Ra by $Ra\cos\phi$, provided pure longitudinal roll motion prevails. Hollands *et al.* (1976) found that the scaling failed, in certain cases, implying a breakdown of the rolls. A stability analysis by Clever & Busse (1977) predicted flow behaviour which was in accord with the heat transfer observations. An experimental study by Ruth *et al.* (1980), henceforth referred to as RHR, established the range of parameters for which scaling occurred, and presented results of a flow visualization study to correlate lack of scaling with flow behaviour. These results permitted a more quantitative comparison with the Clever & Busse predictions.

The reader is referred to RHR for a detailed discussion of the problem, for the experimental conclusions reached, and for the definition of nomenclature used in the present paper (which is an extension of the RHR study). The present contribution reports calculations of velocity components in the longitudinal roll regime and compares the resulting flow pattern with observation. Based on these and other results,

† Present address: Department of Mechanical Engineering, University of Calgary, Alberta, Canada T2N 1N4.

0022-1120/80/4397-8450 $02.00

mechanisms that seem likely to be responsible for the observed behaviour of the flow and heat transfer are postulated and a simple model is formulated which quantitatively correlates the available data.

2. Power-integral analysis for inclined layers

A 'power-integral' technique, similar to that of Stuart (1958) and as applied by Nakagawa (1960) to the horizontal layer, has been used to obtain estimates of the velocities in the longitudinal roll regime. Separating velocity, temperature and pressure into average components (which are sometimes zero) over a given r_3 plane and spatially varying components in the r_2, r_3 plane (where r_3 is the direction normal to the plates, r_2 is the spanwise co-ordinate and r_1 is the upslope co-ordinate directed parallel to the axes of the longitudinal rolls) yields

$$v_1 = v_a(r_3) + A_1 v_1'(r_2, r_3), \tag{1a}$$

$$v_2 = A_2 v_2'(r_2, r_3), \tag{1b}$$

$$v_3 = A_3 v_3'(r_2, r_3), \tag{1c}$$

$$T = T_a(r_3) + A_T T'(r_2, r_3), \tag{1d}$$

and

$$P = P_a(r_3) + A_P P'(r_2, r_3). \tag{1e}$$

In these equations, v_i, T and P are velocity, temperature and pressure, non-dimensionalized respectively by ν/H, ΔT and $\rho g H$. The subscript a denotes an average, the prime a spatially varying component, and the A's denote amplitudes multiplying the spatially varying components. The power-integral technique is applied as follows: the average flow solutions (v_a, T_a and P_a) are found by averaging the governing equations; the functional forms of the primed variables are determined from a linear stability analysis for which the instability is assumed to result in longitudinal rolls; these forms are assumed to persist into the post-critical regime; a nonlinear analysis is then performed to determine the amplitudes. The details of the analytical technique may be found in the thesis by Ruth (1977).

3. The numerical results for air

Profiles for v_a, obtained by means of the power-integral technique, are presented in figure 1, along with selected values from the Galerkin solution of Clever & Busse (1977). The different methods are seen to yield good agreement for $Ra\cos\phi = 1800$ and 2000, but significant discrepancies occur at a value of 5000. The power-integral method also predicts Nusselt numbers within 5% of the measured values up to $Ra\cos\phi = 5000$ if longitudinal rolls prevail, lending additional support to the accuracy of the present predictions well beyond the point of primary instability.

Isovels (contours of equal velocity) for v_1 are presented in figure 2 over the extent of a single roll; negative and positive values refer to velocities directed towards and away from a viewer looking along the r_1 direction through the lower end of the inclined layer. Figure 2(*a*) shows the base flow; for $Ra\cos\phi > 1708$ the clockwise rotation of the roll tends to draw the hot and cold fluid streams into tubular shapes

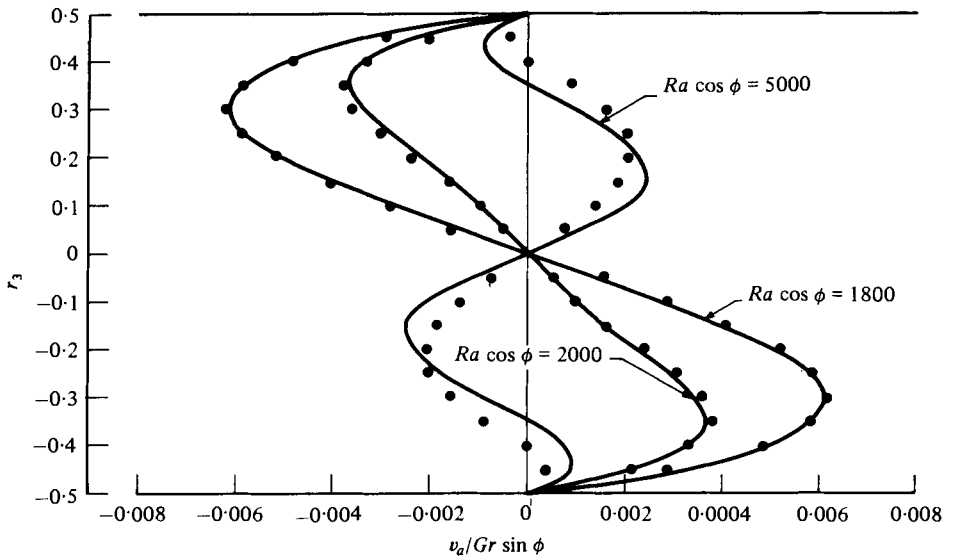

FIGURE 1. Average velocity profiles. —, Present; ●, selected results from Clever & Busse (1977).

with centres that progressively shift their positions with increasing $Ra\cos\phi$. At $Ra\cos\phi \approx 2500$ (figure 2*d*) the 'tube' on the left carrying the warm air up the layer is positioned at about the same elevation as that on the right which returns the cooler fluid down the layer. At $Ra\cos\phi = 5000$ (figure 2*f*) the centre of the warmer stream is substantially higher than that of the cooler.

The numerical predictions also permitted the interpretation of the flow visualization results to be checked. Of particular importance was the verification that the smoke-particle traces in figure 7 of RHR are consistent with the existence of longitudinal rolls, and that the velocities in the spanwise direction, v_2, near the top and bottom of the fluid layer can be very large compared to the upslope v_1 velocities. The importance of these large transverse velocities will be highlighted later.

4. The secondary transition hypothesis

The failure of the heat transfer to scale over certain parameter ranges is directly connected with the breakdown of the longitudinal rolls, i.e. a secondary instability. While most instabilities result in an increase in heat transfer, this instability actually results in a *decrease*. The underlying mechanism is thought to be a shear instability resulting from the relatively high velocity counterflowing streams shown in figure 2. Figure 3 represents the maximum upslope velocities in the 'tubes' by bold arrows facing in alternate directions. The instability resulting from the shear between them would be a cell, idealized as a circle in figure 3, whose axis is perpendicular to the plates (physically the instability is manifest as wavy rolls and unsteadiness). This instability would not augment the heat transfer since it creates motion parallel to the plates rather than across the layer. Furthermore, the motion along the upper arc of the circle in figure 3 moves fluid with positive r_1 and r_3 momentum into a region where both v_1

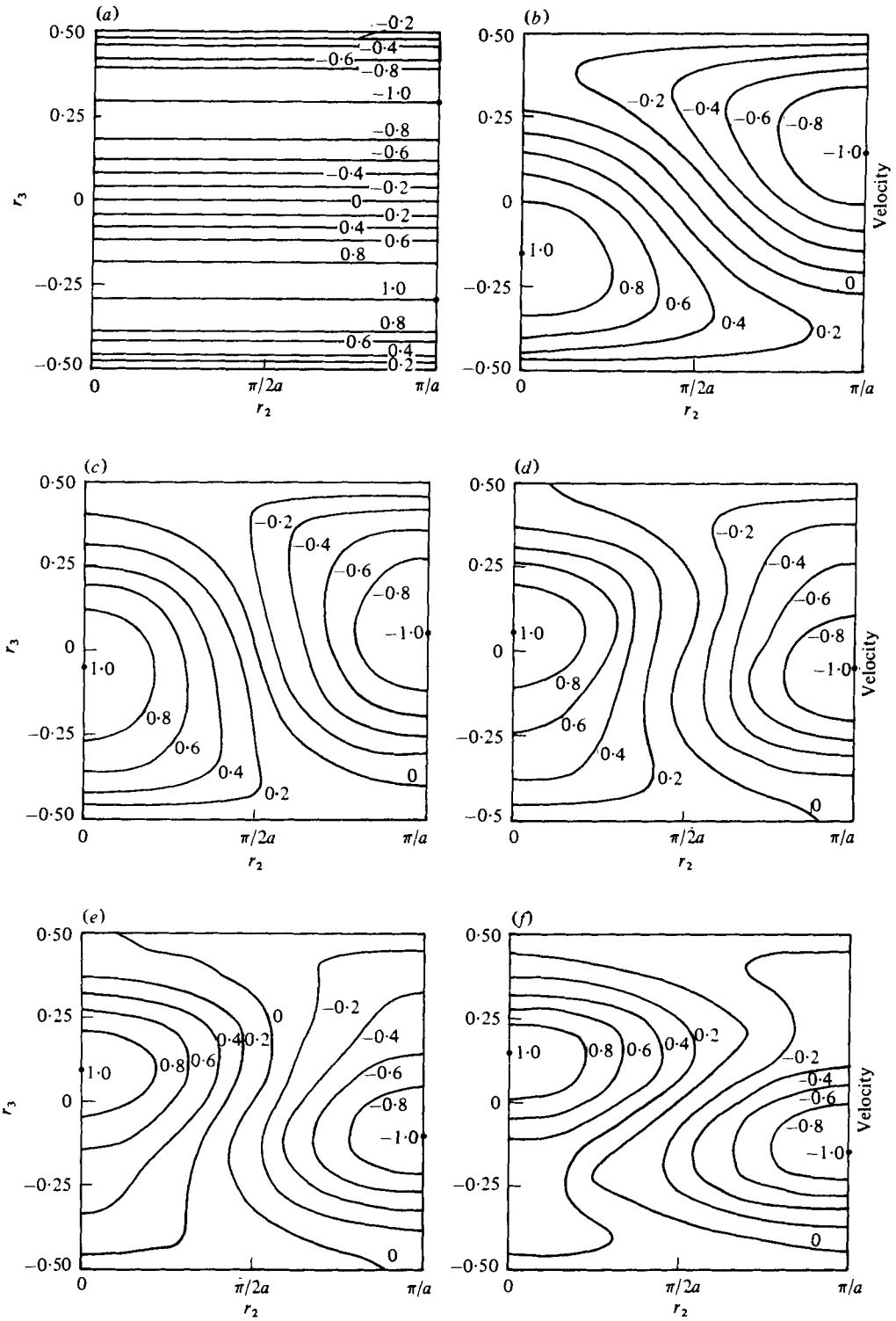

FIGURE 2. Isovels for v_1. Values of $Ra \cos \phi$: (*a*) < 1708; (*b*) 1800; (*c*) 2000; (*d*) 2500; (*e*) 3000; (*f*) 5000.

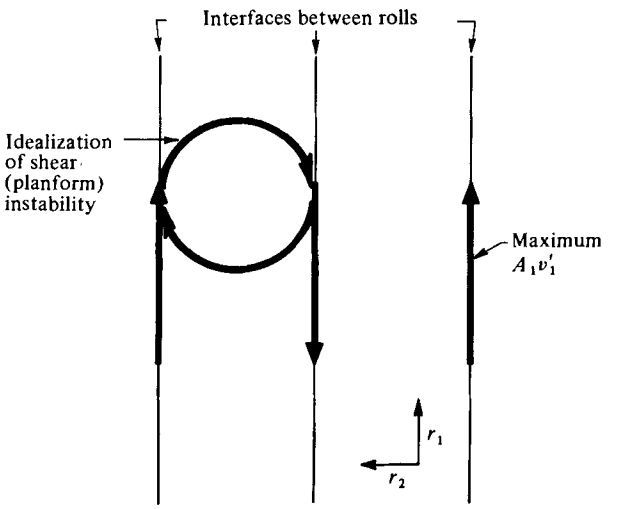

FIGURE 3. The shear (planform) instability.

and v_3 are negative; the opposite occurs on the return arc of the circle. The interference that would result from such motion would actually decrease the v_3 velocities and thus explain also the *decrease* in heat transfer across the layer. The hypothesized instability will be referred to as a planform instability.

Hart (1971), in discussing the transition to wavy vortices in water, proposed a similar mechanism but, after an approximate analysis, concluded that the 'shear forces may be too weak to initiate instability'. In the present study, the visual appearance of the wavy rolls was very similar to Hart's 'wavy vortices', although in some cases the wavy rolls in air, immediately after transition, were not steady whereas the onset of Hart's wavy rolls in water always appeared steady. However, the analysis of Clever & Busse (1977) showed the two phenomena, in air and water, to be of the same general type. Further, Hart identifies the transition to wavy vortices as being 'crucial to the development of violent unsteadiness'. It would therefore appear that the onset of stationary wavy rolls/vortices is a temporary stage in the onset of unsteadiness with this stationary stage persisting over a larger Ra range for water than air. For this reason the steady wavy rolls in air were not always detected. For the purposes of the present paper, it will be assumed that wavy rolls in air and wavy vortices in water are examples of the same mode of instability.

Since the velocity in the present study is scaled by ν/H, it may be interpreted as a Reynolds number, Re; the appropriate Re for a planform instability is therefore given by the maximum value of $A_1 v_1'$. Hart's observations can be used, in conjunction with the analysis of this paper, to estimate the Reynolds number, Re_t, for this transition to wavy vortices. Using Hart's observed Ra's, including his values of the error bars, the transition values of $A_1 v_1'$ (that is Re_t) were calculated from the power-integral analysis. As in Hart's analysis, a Pr of 6·7 was used.

The computed values of Re_t are shown in figure 4. For $\phi \leqslant 45°$ the transition occurs in the range $5 < Re_t < 8$, with $Re_t \simeq 6{\cdot}75$ for four of the angles. The reason for the increase in Re_t for $\phi \geqslant 60°$ is not clear; it may be due to the development of an r_1-temperature gradient at higher angles, or perhaps simply reflects greater uncertainty

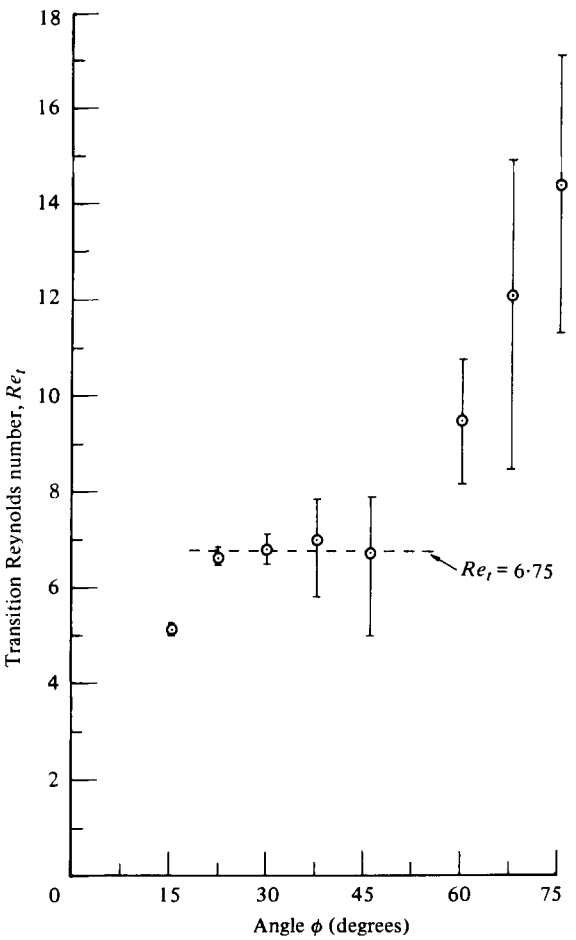

FIGURE 4. Re for onset of waviness (after Hart 1971), $Pr = 6{\cdot}7$.

as suggested by the greatly increased error bounds. These angles are, however, well above those of interest in the present study. Re_t for the planform or wavy instability will be tentatively taken as $Re_t = 6{\cdot}75$.

Returning to the air layer problem, the values of $Re = A_1 v_1'$ from the power-integral analysis have been plotted against $Ra\cos\phi$ for various angles in figure 5. Using the planform instability criterion ($Re_t = 6{\cdot}75$) results in the following conclusions:

(1) the longitudinal rolls would be stable for $\phi = 5°$;

(2) the rolls at $\phi = 10°$ would become unstable at $Ra\cos\phi = 2000$ but would again be stable for $Ra\cos\phi > 5000$;

(3) the rolls will become unstable almost as soon as they appear ($Ra\cos\phi = 1708$). for $\phi \geqslant 15°$.

Some of these results are in agreement with experiment. The rolls at $\phi = 5°$ did remain stable, and the heat transfer scaled, even for Ra values well above $Ra\cos\phi = 1708$. Also, for $\phi > 15°$, unsteadiness was observed, and the heat transfer failed to scale at $Ra\cos\phi$ *very* near 1708, in agreement with figure 5.

There are also points of disagreement which require further explanation. First, the

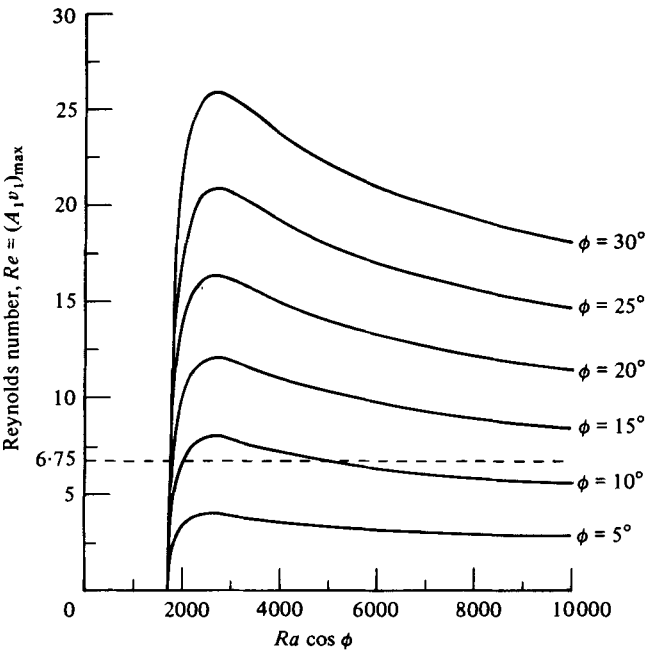

FIGURE 5. Magnitude of Re (maximum value of $A_1 v_r'$), $Pr = 0{\cdot}71$.

instability at $\phi = 10°$ was not observed, and while irregularity in the rolls was observed for $\phi = 15°$, there was no associated suppression in the heat transfer. Furthermore, the heat transfer at $\phi = 20°$ and 25° returned to scaling, suggesting also the return of longitudinal rolls, for $Ra \cos \phi$ well above 1708; these would not be expected on the basis of figure 5. The reasons underlying the suppression of the planform instability and the implied re-establishment of the rolls are now sought.

5. Suppression of instability and re-establishment of rolls

The Reynolds numbers, Re, in figure 5, based on the upslope velocity, increase very rapidly with Ra for values just beyond the first appearance of the rolls. However, the circumferential velocities (v_2 and v_3) also increase, transporting sufficient r_1 momentum between the counterflowing streams to slow the rapid rise of Re and eventually cause it to decrease. Figure 6, showing the ratio of the maximum v_3 velocity to the maximum value of $A_1 v_1'$, illustrates how rapidly the v_3 velocity grows with $Ra \cos \phi$, for various angles.

The large circumferential velocities provide a plausible mechanism for delaying the onset of the planform instability, and for re-establishing the longitudinal rolls at $Ra \cos \phi$ values higher than those at which the instability occurred. When the angular momentum of the flow increases in the direction of the radius of curvature of the flow, as it does here, the balance of centrifugal and pressure forces exert a strong stabilizing influence. Bradshaw (1969) provides a clear insight into the mechanisms involved, and draws the analogy with the effect of a stable density stratification. The simplest possible model for restabilization would assert that this effect begins to play a

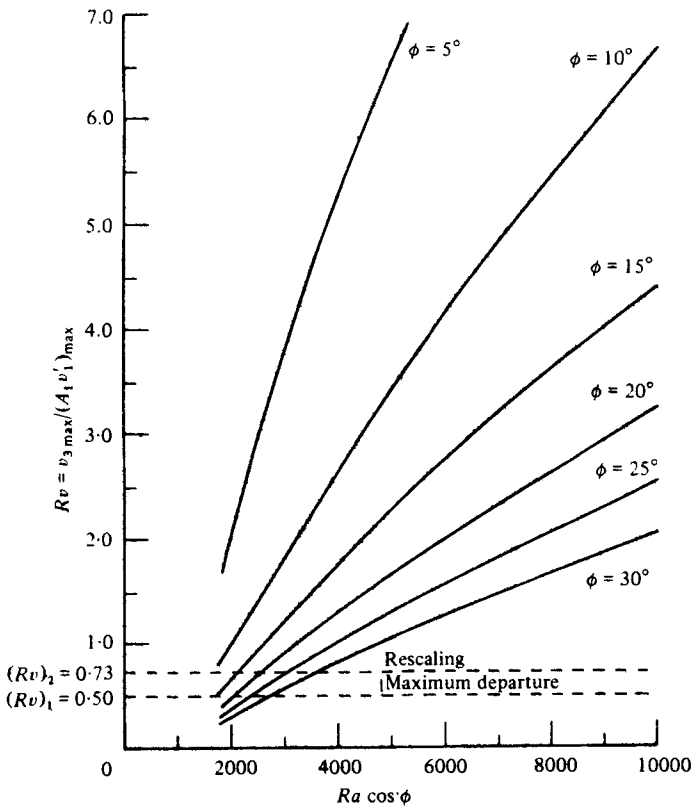

FIGURE 6. The ratio Rv.

significant role at a certain ratio of $v_3/A_1 v_1' = (Rv)_1$, and completely overwhelms the shear instability at a somewhat higher ratio, $(Rv)_2$. It remains to determine appropriate values of $(Rv)_1$ and $(Rv)_2$.

Estimates can be obtained by plotting the difference between the measured Nusselt number, Nu, and the value that would be obtained if pure longitudinal rolls existed, Nu_t, against $Ra\cos\phi$, for $\phi = 20°$, 25° and 30°. Figure 7 shows these results using the RHR data. Very near $Ra\cos\phi = 1708$, Nu falls rapidly below Nu_t with increasing Ra, but each curve passes through a minimum referred to here as the 'maximum departure from scaling', which is associated with the $(Rv)_1$ ratio. Table 1 indicates $Ra\cos\phi$ values corresponding to each minimum and using these values in figure 6, permits the corresponding Rv values to be found. These Rv values are also tabulated in table 1. The point of maximum departure from scaling lies quite consistently around an Rv of 0·5; thus $(Rv)_1 = 0{\cdot}5$ is assumed.

At larger $Ra\cos\phi$, the heat transfer 'returns to scaling' (that is, $Nu - Nu_t \approx 0$) for $\phi = 20°$ and 25° at values indicated in table 1. Using these in figure 6 yields the Rv values in the table, which lie near 0·73; thus $(Rv)_2 \approx 0{\cdot}73$ is assumed.

This mechanism with these Rv values will certainly describe the re-establishment of scaling. It also removes the other sources of disagreement between the data and the planform instability model described in the previous section. For example, for $\phi = 10°$, figure 5 suggests that a shear instability should occur at $Ra\cos\phi = 2000$, but figure 6

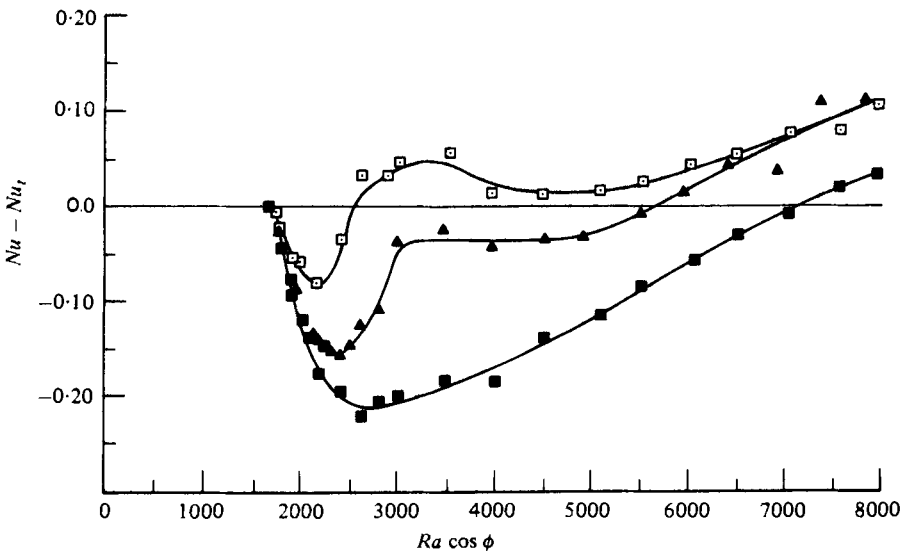

FIGURE 7. The departure from scaling: □, 20°; ▲, 25°; ■, 30°.

	Point of maximum non-scaling		Point of return to scaling	
Angle	$Ra\cos\phi$	Rv	$Ra\cos\phi$	Rv
20°	2050–2250	0·513–0·597	2500–2700	0·701–0·783
25°	2300–2500	0·483–0·547	2900–3200	0·675–0·768
30°	2500–2900	0·442–0·545		

TABLE 1. The stabilizing mechanism

indicates that Rv is already 1·0 at this point, so that the stabilizing effect of the circumferential velocities never permits the instability to occur. For $\phi = 15°$, Rv is 0·55 at $Ra\cos\phi = 1800$, suggesting that the circumferential velocities also play a significant, but not dominating, roll, consistent with observed marginal stability of the flow.

As $Ra\cos\phi$ increases well beyond the value required for the re-establishment of the longitudinal rolls, another type of instability occurs. This was observed in RHR as a change in the spatial wavenumber, followed by unsteady motion at still higher Ra values. The present model does not deal with this higher-order instability.

6. Comparisons between experiments, the present theory and the work of Clever & Busse

Figure 8 presents a comparison between the present model, the theory of Clever & Busse, and the visually observed flow regimes reported in RHR. The area to the left of $Ra\cos\phi = 1708$ is the stable base flow regime. The area below the 'experimental' curve corresponds to the region where stable longitudinal rolls were observed, while the rolls in the area above the curve exhibited waviness and/or unsteadiness. With increasing $Ra\cos\phi$, the experimental curve plunges sharply downward very near

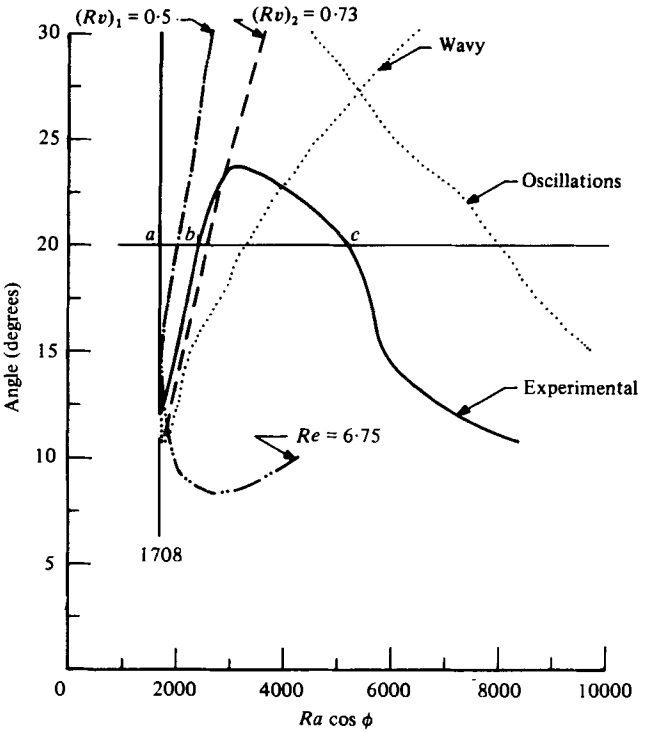

FIGURE 8. A comparison of visual and theoretical results. · · · · ·, Clever & Busse (1977); ——, experiments of Ruth *et al.* (1980); — · —, — · · —, — —, present results.

$Ra\cos\phi = 1708$ ($12{\cdot}5 \leqslant \phi \leqslant 30$), ascends in the range $1708 \leqslant Ra\cos\phi \leqslant 3100$ and again gradually descends for $Ra\cos\phi \geqslant 3100$. The changes can be best understood by imagining $Ra\cos\phi$ to be increased at a fixed angle (e.g. $\phi = 20°$ as shown in figure 8). At point *a*, just slightly past $Ra\cos\phi = 1708$, the planform (or wavy) instability associated with the suppression in heat transfer sets in. At *b*, steady longitudinal rolls are again established, but these become unsteady again at *c*.

The model presented in this paper deals only with the planform instability and the restabilization. According to the model, points in figure 8 lying above the $Re = 6{\cdot}75$ curve have sufficient upslope v_1 velocities to cause a shear instability (for $\phi > 15°$, note that the $Re = 6{\cdot}75$ curve coincides with the near-vertical experimental curve). Thus, for the $\phi = 20°$ line, the $Re = 6{\cdot}75$ curve is crossed just past $Ra\cos\phi = 1708$, thereby predicting the onset of the planform instability. Increasing Ra further causes the v_2 and v_3 velocities to increase to the point that the increased suppression of the heat transfer is halted at $(Rv)_1 = 0{\cdot}5$. At $(Rv)_2 = 0{\cdot}73$, v_2 and v_3 dominate completely, re-establishing the longitudinal rolls and causing the heat transfer to scale.

The analysis of Clever & Busse also predicts the wavy or planform instability to occur for $Ra\cos\phi$ just above 1708 (for $\phi \geqslant 11°$), followed by a return to longitudinal rolls. The predicted values of $Ra\cos\phi$ for the return of longitudinal rolls are up to 50 % higher than observed. In discussing their comparison with Hart's data, Clever & Busse suggested that the disagreement perhaps resulted from the time delay for the instability to become visible. This is unlikely to be the reason for the present disagreement since the instabilities in air set in much more rapidly.

The analysis of Clever & Busse was more extensive than that provided here in that they also presented predictions for the oscillatory instability. Again, good agreement between the trends of the present observations and their predictions are evident, with even the inflexion points in the curves being reproduced. However, the predicted values of $Ra\cos\phi$ are approximately 60 % higher than the observed values.

It is also noted that Clever & Busse predict values of the secondary instability at larger $Ra\cos\phi$ than were observed in the air layer, whereas the opposite occurred when Hart's data were used. This may suggest that the discrepancy is associated with the temperature gradient in the upslope direction, which was ignored in the Clever & Busse analysis. However, this gradient will be small at the lower angles of inclination.

7. Conclusions

(1) A theoretical study based on the power-integral technique has been used to give estimates of the upslope convection velocities. For $Ra\cos\phi < \sim 5000$, the results correlate well with previously reported flow visualization observations.

(2) The analysis has confirmed the average upslope velocity profiles reported by Clever & Busse (1977), although small discrepancies do develop as $Ra\cos\phi$ increases.

(3) Based on the analytical results, the secondary transition hypothesis, advanced in RHR, has been associated with the shear or planform instability first suggested by Hart (1971).

(4) A stabilizing mechanism which counteracts the planform instability has been proposed. The combined effects of the destabilizing–stabilizing model have been used to correlate the heat transfer experiments and the flow visualization results of RHR.

(5) The physical arguments presented in this paper and the experimental data presented in RHR are in good qualitative agreement with the theoretical predictions of Clever & Busse (1977).

This work was supported by an operating grant from the National Research Council of Canada. As well, the first author was supported by a National Research Council of Canada Post-Graduate Scholarship. Both grants are acknowledged with gratitude. The authors would like to thank Dr F. H. Busse and Dr R. M. Clever for providing an expanded version of their results which made detailed comparisons with their work possible.

REFERENCES

Bradshaw, P. 1969 The analogy between streamline curvature and buoyancy in turbulent shear flow. *J. Fluid Mech.* **36**, 177–191.

Clever, R. M. 1973 Finite amplitude longitudinal convection rolls in an inclined layer. *Trans. A.S.M.E. J. Heat Transfer* **95**, 407–408.

Clever, R. M. & Busse, F. H. 1977 Instabilities of longitudinal convection rolls in an inclined layer. *J. Fluid Mech.* **81**, 107–127.

Hart, J. E. 1971 Transition to a wavy vortex regime in convective flow between inclined plates. *J. Fluid Mech.* **48**, 265–271.

Hollands, K. G. T., Unny, T. E., Raithby, G. D., & Konicek, L. 1976 Free convective heat transfer across inclined air layers. *Trans. A.S.M.E. J. Heat Transfer* **98**, 189–193.

Nakagawa, Y. 1960 Heat transport by convection. *Phys. Fluids* **3**, 82–86.

RUTH, D. W. 1977 On free convection by longitudinal rolls in inclined infinite air layers heated from below. Ph.D. Thesis, University of Waterloo.

RUTH, D. W., HOLLANDS, K. G. T. & RAITHBY, G. D. 1980 On free convection experiments in inclined air layers heated from below. *J. Fluid Mech.* **96**, 461–479.

STUART, J. T. 1958 On the non-linear mechanics of hydrodynamic stability. *J. Fluid Mech.* **4**, 1–21.